Inorg. Chem. **2007**, *46*, 10261–10267

A Series of Lanthanide–Transition Metal Frameworks Based on 1-, 2-, and 3D Metal–Organic Motifs Linked by Different 1D Copper(I) Halide Motifs

Jian-Wen Cheng,[†] Shou-Tian Zheng,[†] and Guo-Yu Yang*[,†,‡]

State Key Laboratory of Structural Chemistry, Fujian Institute of Research on the Structure of Matter, and Graduate School of the Chinese Academy of Sciences, Fuzhou, Fujian 350002, China, and State Key Laboratory of Rare Earth Materials and Applications, Peking University, Beijing 100871, China

Received July 24, 2007

Hydrothermal reactions of lanthanide(III) oxide and copper halide with isonicotinic acid (Hina) and pyridine-2,3-dicarboxylic acid (H_2pdc) or 1,2-benzenedicarboxylic acid (H_2bdc) lead to three novel lanthanide(III)–copper(I) heterometallic compounds, namely, $[Ce_2(ina)_5(na)_2(H_2O)_2][Cu_5Br_4]$ (**1**, na = nicotinic acid), $[Er_4(ina)_8(bdc)_2(OH)(H_2O)_5][Cu_8I_7]$ (**2**), and $[Ce_3(ina)_8(bdc)(H_2O)_4][Cu_7Br_6]$ (**3**). Compound **1** is constructed from two distinct units of the Ln–organic double chains and inorganic $[Cu_5Br_4]_n^{n+}$ chains. Compound **2** consists of 2D Ln–organic layers and 1D $[Cu_8I_7]_n^{n+}$ cluster chains. Compound **3** can be viewed as a 1D $[Cu_6Br_6]_n$ chainlike motif inserted into the channels of a 3D Ln–Cu–organic motif. Compounds **1**–**3** exhibit three different 1D inorganic copper(I)–halide chains interconnected with metal–organic 1D chains, 2D layers, and 3D nets resulting in three mixed-motif non-interpenetrating heterometallic Cu–halide–lanthanide (Ln)–organic frameworks, which represent good examples and a facile method to construct such mixed-motif heterometallic compounds. Furthermore, the IR, TGA, and UV–vis spectra of **1**–**3** were also studied.

Introduction

The current increasing interest in metal−organic frameworks not only stems from their potential applications in optoelectronic, magnetic, and porous materials but also from their intriguing variety of topologies and motifs.[1−3] Although a large number of frameworks with various structure motifs have been reported, the architectures formed by two different motifs, on the other hand, are still less well investigated. Some mixed-motif interpenetrating networks such as 1D/2D inclined interpenetration, 1D/3D interpenetration, 2D/3D parallel interpenetration, 2D/2D inclined interpenetration of (4,4) and (6,3) sheets, 3D/3D interpenetration of two diamond nets, and one NbO net have been shown by the two comprehensive reviews by Batten and Robson.[4] Non-interpenetrating examples, such as different 1D molybdenum oxide anionic chains link cationic 1D, 2D, and 3D copper−organic nets, have been reported by Zubieta.[5] To design such non-interpenetrating mixed-motif compounds, Loye[6] brought up a reasonable approach by using two different transition metals (TMs); the unique coordination preferences of two dissimilar metals could lead to new frameworks with each metal keeping its own structural motif. To date, most of the work has focused on the assembly of mixed TMs.[5,6] Although

* To whom correspondence should be addressed. E-mail: ygy@fjirsm.ac.cn. Fax: (+86) 591-8371-0051.

† Fujian Institute of Research on the Structure of Matter and Graduate School of the Chinese Academy of Sciences.

‡ Peking University.

(1) (a) Plečnik, C. E.; Liu, S.; Shore, S. G. *Acc. Chem. Res.* **2003**, *36*, 499. (b) Lombardi, J. R.; Davis, B. *Chem. Rev.* **2002**, *102*, 2431. (c) Benelli, C.; Gatteschi, D. *Chem. Rev.* **2002**, *102*, 2369. (d) Sakamoto, M.; Manseki, K.; Ōkawa, H. *Coord. Chem. Rev.* **2001**, *219*−*221*, 379.

(2) (a) Ockwig, N. W.; Delgado-Friedrichs, O.; O'Keeffe, M.; Yaghi, O. M. *Acc. Chem. Res.* **2005**, *38*, 176. (b) Férey, G.; Mellot-Draznieks, C.; Serre, C.; Millange, F. *Acc. Chem. Res.* **2005**, *38*, 217. (c) Hill, R. J.; Long, D. L.; Champness, N. R.; Hubberstey, P.; Schröder, M. *Acc. Chem. Res.* **2005**, *38*, 335.

(3) (a) Rao, C. N. R.; Natarajan, S.; Vaidhyanathan, R. *Angew. Chem., Int. Ed.* **2004**, *43*, 1466. (b) Blatov, V. A.; Carlucci, L.; Ciani, G.; Proserpio, D. M. *CrystEngComm* **2004**, *6*, 377. (c) Kitagawa, S.; Kitaura, R.; Noro, S. I. *Angew. Chem., Int. Ed.* **2004**, *43*, 2334.

(4) (a) Batten, S. R.; Robson, R. *Angew. Chem., Int. Ed.* **1998**, *37*, 1460. (b) Batten, S. R. *CrystEngComm* **2001**, *3*, 67 and the website therein.

(5) (a) Hagrman, D.; Zubieta, C.; Rose, D. J.; Zubieta, J.; Haushalter, R. C. *Angew. Chem., Int. Ed.* **1997**, *36*, 873. (b) Hagrman D.; Zubieta, J. *Chem. Commun.* **1998**, 2005. (c) Hagrman, P. J.; Bridges, C.; Greedan, J. E.; Zubieta, J. *J. Chem. Soc., Dalton Trans.* **1999**, 2901.

(6) Ciurtin, D. M.; Smith, M. D.; zur Loye, H. C. *Chem. Commun.* **2002**, 74.

10.1021/ic701468q CCC: $37.00
Published on Web 11/01/2007

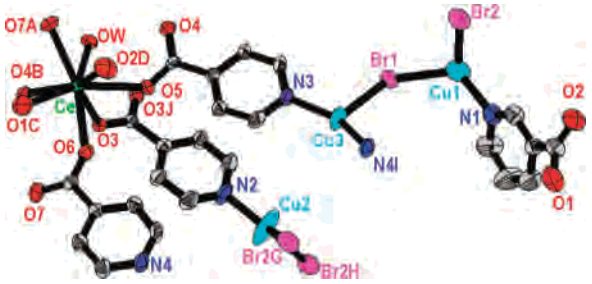

Figure 1. The coordination environments of Ce and Cu atoms in **1**. Symmetry codes for the generated atoms are the same as Table 2.

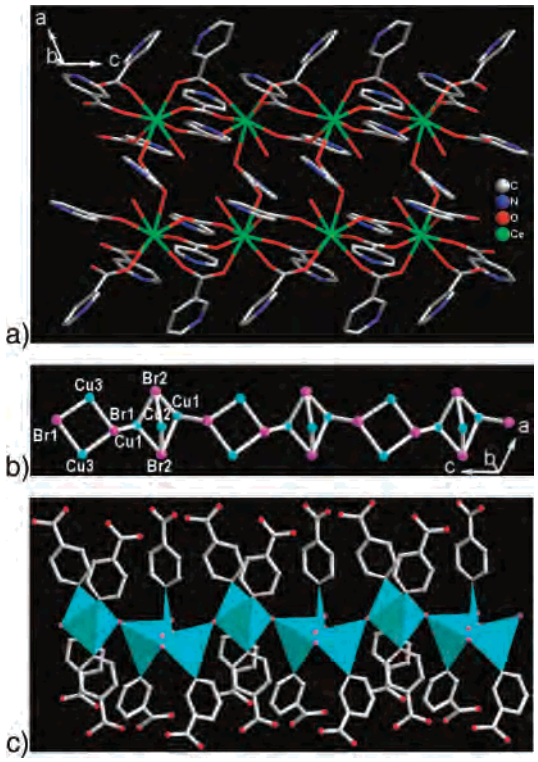

Figure 2. (a) Ln−organic double chain motif in **1**. (b) Inorganic $[Cu_5Br_4]_n^{n+}$ chains along the *c*-axis. (c) Polyhedral view of the 1D $[Cu_5Br_4N_7]_n^{n+}$ chains.

a number of Ln−TM metal−organic frameworks have been reported due to their fascinating structural topologies and potential applications,[7−8] the frameworks based on linkages of Ln−organic motifs and TM−halide motifs by organic ligands are still only rarely reported.

The coordination chemistry of the copper(I) halides (CuX, X = Cl/Br/I) has been of great interest for their large structural variation and rich electronic and optical properties.[9] In a search of the Cambridge Structural Database (using ConQuest Version 1.9, updated Jan 2007), more than 1000 oligomeric and polymeric inorganic CuX cluster or cluster polymer substructures such as dimers, tetramers of cubane and stepped cubane types, single, double, and multiple chains, and 2D layers have been well documented,[9−10] while the constrution of CuX−Ln heterometallic compounds and their physical properties remains less developed. Therefore, the introduction of a CuX motif into the Ln−organic frameworks not only provides a rational synthetic strategy for unusual architectures but also opens the way to make new materials.

To make mixed-motif non-interpenetrating heterometallic frameworks, our strategy is introducing CuX into the Ln organic framework on the basis of the characteristics of Ln and Cu ions with different affinity for O-, N-, and X-donors. Recently, we reported that CuX can form different clusters in Ln−organic frameworks.[11] The rich structural motif of CuX encourages us to continue our search for new CuX−Ln−organic compounds. Here we present systematic formation of three novel mixed-motif non-interpenetrating CuX−Ln−organic frameworks obtained by hydrothermal reactions of Ln_2O_3, $CuBr_2$/CuI, isonicotinic acid (Hina), and pyridine-2,3-dicarboxylic acid (H_2pdc)/1,2-benzenedicarboxylic acid (H_2bdc) in water in the presence of $HClO_4$ (pH 2): $[Ce_2(ina)_5(na)_2(H_2O)_2][Cu_5Br_4]$ (**1**, na = nicotinic acid); $[Er_4(ina)_8(bdc)_2(OH)(H_2O)_5][Cu_8I_7]$ (**2**); $[Ce_3(ina)_8(bdc)(H_2O)_4][Cu_7Br_6]$ (**3**). The frameworks of **1**−**3** exhibit three different 1D inorganic CuX chains linking to distinct Ln−organic motifs, 1D chains, 2D layers, and 3D nets, respectively.

Experimental Section

Materials and Methods. All chemicals were purchased commercially and used without further purification. Elemental analyses for C, H, and N were performed on a Vario EL III elemental analyzer. The FT-IR spectra (KBr pellets) were recorded on an ABB Bomen MB 102 spectrometer, and the UV/vis spectra on a Lambda900 spectrophotometer. Thermogravimetric analyses were performed on a Mettler TGA/SDTA 851e analyzer with a heating rate of 10 °C/min under an air atmosphere.

$[Ce_2(ina)_5(na)_2(H_2O)_2][Cu_5Br_4]$ (1). A mixture of CeO_2 (0.174 g), $CuBr_2$ (0.045 g), Hina (0.246 g), H_2pdc (0.168 g), H_2O (10 mL), and $HClO_4$ (0.385 mmol) was sealed in a 30 mL Teflon-lined bomb at 170 °C for 7 days and then cooled to room temperature. Yellow prismatic crystals of **1** were obtained (yield: 15% based on $CuBr_2$). Anal. Calcd for **1**, $C_{42}H_{32}Br_4Cu_5Ce_2N_7O_{16}$: C, 27.90; H, 1.78; N, 5.42. Found: C, 27.75; H, 2.18; N, 5.32. IR bands (cm^{-1}) for **1**: 3452 s, 1598 vs, 1548 m, 1406 vs, 867 w, 850 w, 775 m, 759 m, 705 m, 547 w.

$[Er_4(ina)_8(bdc)_2(OH)(H_2O)_5][Cu_8I_7]$ (2). A mixture of Er_2O_3 (Er_2O_3, 0.191 g), CuI (0.0528 g), Hina (0.246 g), H_2bdc (0.147 g), H_2O (10 mL), and $HClO_4$ (0.385 mmol) was sealed in a 30 mL Teflon-lined bomb at 170 °C for 7 days and then cooled to room temperature. Yellow prismatic crystals of **2** were obtained (yield:

(7) (a) Plečnik, C. E.; Liu, S. M.; Shore, S. G. *Acc. Chem. Res.* **2003**, *36*, 499. (b) Sun, Y.-Q.; Zhang, J.; Yang, G.-Y. *Chem. Commun.* **2006**, 4700. (c) Sun, Y.-Q.; Yang, G.-Y. *Dalton Trans.* **2007**, 3771. (d) Cahill, C. L.; de Lill, D. T.; Frisch. M. *CrystEngComm* **2007**, *9*, 15. (e) Cheng, J.-W.; Zheng, S.-T.; Yang, G.-Y. *Dalton Trans.* **2007**, 4059.
(8) (a) He, Z.; He, C.; Gao, E.; Wang, Z.; Yang, X.; Liao, C.; Yan, C. H. *Inorg. Chem.* **2003**, *42*, 2206. (b) Shi, W.; Chen, X.; Zhao, Y.; Zhao, B.; Cheng, P.; Yu, A.; Song, H.; Wang, H.; Liao, D.; Yan, S.; Jiang, Z. *Chem.—Eur. J.* **2005**, *11*, 5031. (c) Yang, J.; Yue, Q.; Li, G.; Li, G.; Chen, J. *Inorg. Chem.* **2006**, *45*, 2857. (d) Shi, W.; Chen, X.; Zhao, B.; Yu, A.; Song, H.; Cheng, P.; Wang, H.; Liao, D.; Yan, S. *Inorg. Chem.* **2006**, *45*, 3949.
(9) (a) Mitzi, D. B. *Prog. Inorg. Chem.* **1999**, *48*, 1. (b) Vitale, M.; Ford, P. C. *Coord. Chem. Rev.* **2001**, *219−221*, 3. (c) Lu, J. Y. *Coord. Chem. Rev.* **2003**, *246*, 327.
(10) (a) Blake, A. J.; Brooks, N. R.; Champness, N. R.; Cooke, P. A.; Deveson, A. M.; Fenske, D.; Hubberstey, P.; Li, W. S.; Schröder, M. *J. Chem. Soc., Dalton Trans.* **1999**, 2103. (b) Li, G.; Shi, Z.; Liu, X.; Dai, Z.; Feng, S. *Inorg. Chem.* **2004**, *43*, 6884.
(11) (a) Zhang, M.-B.; Zhang, J.; Zheng, S.-T.; Yang, G.-Y. *Angew. Chem., Int. Ed.* **2005**, *44*, 1385. (b) Cheng, J.-W.; Zhang, J.; Zheng, S.-T.; Zhang, M.-B.; Yang, G.-Y. *Angew. Chem., Int. Ed.* **2006**, *45*, 73.

Table 1. Crystal Data and Structure Refinement for Compounds **1**−3

param	**1**	**2**	**3**
formula	$C_{42}H_{32}Br_4Cu_5Ce_2N_7O_{16}$	$C_{64}H_{51}I_7Cu_8Er_4N_8O_{30}$	$C_{56}H_{44}Br_6Cu_7Ce_3N_8O_{24}$
M_r	1808.33	3477.79	2557.59
crystal system	monoclinic	triclinic	monoclinic
space group	*C*2/*c*	$P\bar{1}$	$P2_1/c$
a (Å)	17.3097(13)	14.9613(2)	10.1130(5)
b (Å)	32.694(2)	15.8582(4)	19.6280(8)
c (Å)	9.8565(7)	18.5100(8)	34.4168(16)
α (deg)	90.00	86.332(7)	90.00
β (deg)	114.494(3)	83.536(6)	92.380(3)
γ (deg)	90.00	72.881(5)	90.00
V (Å^3)	5076.1(6)	4168.2(2)	6825.8(5)
Z	4	2	4
D_c (g cm^{-3})	2.366	2.771	2.489
μ (mm^{-1})	*7.034*	*8.649*	*7.687*
F(000)	*3448*	*3212*	*4860*
GOF	1.087	1.109	1.101
collcd reflcns	19 659	32 517	52 120
unique reflcns (R_{int})	5818 (0.0434)	18 851 (0.0332)	15 618 (0.0586)
obsd reflcns [$I > 2\sigma(I)$]	5010	15 230	12 768
refined params	354	1090	946
$R_1{}^a$/$wR_2{}^b$ [$I > 2\sigma(I)$]	0.0537/0.1284	0.0507/0.0889	0.0647/0.1604
$R_1{}^a$/$wR_2{}^b$ (all data)	0.0647/0.1351	0.0674/0.0981	0.0819/0.1727

[a] $R_1 = \Sigma||F_o| - |F_c||/\Sigma|F_o|$. [b] $wR_2 = \{\Sigma[w(F_o^2 - F_c^2)^2]/\Sigma[w(F_o^2)^2]\}^{1/2}$.

10% based on CuI). Anal. Calcd for **2**, $C_{64}H_{51}I_7Cu_8Er_4N_8O_{30}$: C, 22.10; H, 1.48; N, 3.22. Found: C, 21.93; H, 1.91; N, 3.03. IR bands (cm^{-1}) for **2**: 3450 s, 1595 vs, 1548 m, 1435 vs, 1408 w, 860 w, 769 m, 681 m.

$[Ce_3(ina)_8(bdc)(H_2O)_4][Cu_7Br_6]$ (3). Compound **3** was synthesized by a procedure similar to that of **1**, except that H_2pdc was replaced by H_2bdc (0.147 g). Yellow prismatic crystals of **3** were obtained (yield: 23% based on $CuBr_2$). Anal. Calcd for **3**, $C_{56}H_{44}Br_6Cu_7Ce_3N_8O_{24}$: C, 26.30; H, 1.73; N, 4.38. Found: C, 26.32; H, 2.15; N, 4.43. IR bands (cm^{-1}) for **3**: 3444 s, 1599 vs, 1544 s, 1417 vs, 1220 w, 1056 w, 868 w, 774 m, 707 m, 694 m, 651 w.

Single-Crystal Structure Determination. The intensity data were collected on Mercury CCD diffractometer with graphite-monochromated Mo Kα radiation (λ = 0.710 73 Å) at room temperature. All absorption corrections were performed using the multiscan program. The structure were solved by direct methods and refined by full-matrix least-squares on F^2 with the SHELXTL-97 program.[12] The H atoms of organic ligands were geometrically placed and refined using a riding model. However, the H atoms of water molecules in **1**−**3** and hydroxy H atoms in **2** have not been included in the final refinement. All atoms except for hydrogen atoms were refined anisotropically. Br2/Br2′ in **1** and Cu2/Cu2′ in **3** are disordered. O25 in **2** is protonated for charge balance, as confirmed by the bond valence sum (BVS) for O25 being 1.16. Further details for structural **1**−**3** analyses are summarized in Table 1, and selected bond lengths of compounds **1**−**3** are listed in Tables 2−4. CCDC-644694−644696 for **1**−**3** contain the crystallographic data in CIF format.

Results and Discussion

Structure of 1. 1 is constructed from Ln−organic double chains and inorganic $[Cu_5Br_4]_n^{n+}$ chains both parallel to the *c*-axis. The asymmetric unit of **1** contains one unique Ce^{3+}, three Cu^+, two Br^- ions, one na ligand, and two half ina ligands (Figure S1). The Ce^{3+} ion is eight-coordinate and has bicapped trigonal prism coordination environments: one water molecule and seven carboxylate oxygen atoms (O_{COO^-}) from five ina ligands and two na ligands (Figures 1 and S1). The Ce−O bond lengths range from 2.412(5) to 2.644(5) Å (Table 2). The Ce^{3+} ions are bridged by exo-bidentate carboxyl groups of ina and na ligands to form a double chain motif (Figure 2a). Interestingly, decarboxylation occurred in the ortho position and pdc was transformed into na under hydrothermal conditions,[13] which induce the Ln−organic part into a low-dimensional double chain motif.

Table 2. Selected Bond Lengths (Å) for **1**[a]

Ce−O(7A)	2.412(5)	Cu(1)−Cu(1F)	2.739(3)
Ce−O(4B)	2.424(5)	Cu(1)−Br(2)	2.830(7)
Ce−O(1C)	2.438(6)	Cu(2)−N(2)	1.957(9)
Ce−O(6)	2.444(5)	Cu(2)−Br(2G)	2.349(7)
Ce−O(5)	2.453(5)	Cu(2)−Br(2H)	2.349(7)
Ce−O(2D)	2.506(5)	Cu(2)−Cu(1G)	2.541(2)
Ce−O(3)	2.598(4)	Cu(2)−Cu(1H)	2.541(2)
Ce−OW	2.644(5)	Cu(2)−Br(2H)	2.5683(19)
Cu(1)−N(1)	2.003(7)	Cu(2)−Br(2G)	2.5683(18)
Cu(1)−Br(2)	2.461(2)	Cu(3)−N(4I)	1.951(6)
Cu(1)−Br(1)	2.4758(16)	Cu(3)−N(3)	1.966(6)
Cu(1)−Cu(2E)	2.541(2)	Cu(3)−Br(1)	2.5862(14)
Cu(1)−Br(2F)	2.701(2)	Cu(3)−Br(1H)	2.7965(16)

[a] Symmetry codes: (A) $x, -y, z - 1/2$; (B) $x, -y, z + 1/2$; (C) $-x + 1/2, y - 1/2, -z - 1/2$; (D) $-x + 1/2, -y + 1/2, -z - 1$; (E) $x, y, z - 1$; (F) $-x + 1, y, -z - 3/2$; (G) $x, y, z + 1$; (H) $-x + 1, y, -z - 1/2$; (I) $-x + 1/2, -y + 1/2, -z$; (J) $-x + 1, y, -z + 1/2$; (K) $-x + 1/2, y + 1/2, -z - 1/2$.

The inorganic motif consists of unique 1D $[Cu_5Br_4]_n^{n+}$ chains comprising three unique Cu^+ and two Br^- ions. Both Cu(1) and Cu(3) atoms are four-coordinated in distorted tetrahedral geometries, $Cu(1)Br_3N$ and $Cu(3)Br_2N_2$, while Cu(2) is three-coordinated in a trigonal plane, $Cu(2)Br_2N$. The Cu^+ ions are linked by μ_3-Br to give two types of small cluster cores: a trinuclear $[Cu_3Br_2]^+$ core containing one Cu(2) and two Cu(1) atoms; a dimeric $[Cu_2Br_2]$ core containing

(12) (a) Sheldrick, G. M. *SHELXS97, Program for Crystal Structure Solution*; University of Göttingen: Göttingen, Germany, 1997. (b) Sheldrick, G. M. *SHELXL97, Program for Crystal Structure Refinement*; University of Göttingen: Göttingen, Germany, 1997.

(13) Chen, W.; Yuan, H.; Wang, J.; Liu, Z.; Xu, J.; Yang, M.; Chen, J. *J. Am. Chem. Soc.* **2003**, *125*, 9266.

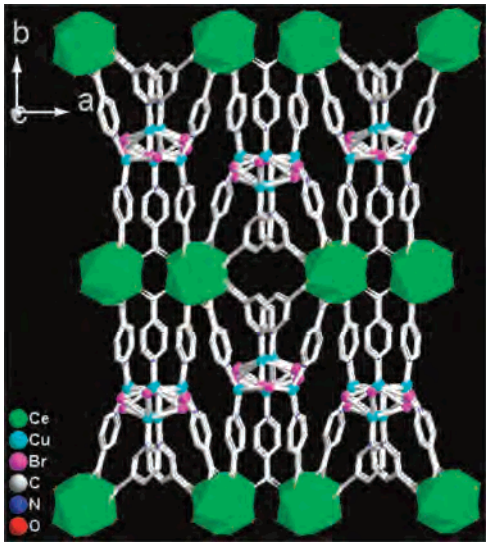

Figure 3. Framework of **1** viewed down the approximate [001] direction.

Scheme 1. Coordination Modes of the Ligands in **1** (a, c), **2** (a, b, d), and **3** (a, e)

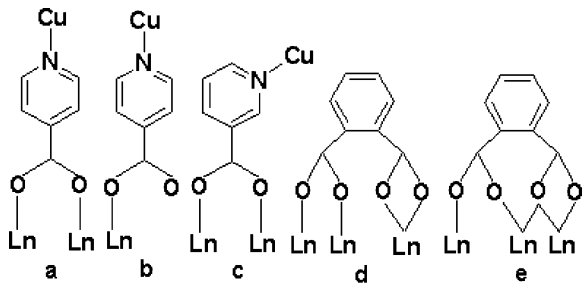

two Cu(3) atoms. The $[Cu_3Br_2]^+$ and $[Cu_2Br_2]$ cores share one μ_3-Br(1) to form a cationic chain of $[Cu_5Br_4]_n^{n+}$ (Figure 2b,c). Hence, the connection between the Ln−organic motifs and the inorganic motifs via Cu−N bonds gives a 3D covalent famework (Figure 3).

Structure of 2. The framework **2** consists of 2D Ln−organic motifs and 1D inorganic $[Cu_8I_7]_n^{n+}$ motifs. The asymmetric unit of **2** contains four Er^{3+}, eight Cu^+, and seven I^- ions, two bdc ligands, and eight ina ligands with two different coordination modes (Figure S2 and Scheme 1). Er(1) and Er(4) atoms are seven-coordinate with distorted capped trigonal prism geometries: two water molecules, three O_{COO}^- from three ina ligands, two O_{COO}^- from two bdc ligands for Er(1); one μ_2-OH, four O_{COO}^- from four ina ligands, two O_{COO}^- from one bdc ligand for Er(4). Er(2) and Er(3) are eight-coordinate with bicapped trigonal prism configrations: two water molecules, five O_{COO}^- from five ina ligands, one O_{COO}^- from one bdc ligand for Er(2); two water molecules and one μ_2-OH, two O_{COO}^- from two ina ligands, three O_{COO}^- from two bdc ligands for Er(3) (Figure 4, S2). The Er−O bond lengths range from 2.202(6) to 2.612(6) Å (Table 3). The Er atoms are linked up via both μ_2-OH and O_{COO} groups of ina and bdc ligands to give rise to 2D layered motif along the *ab* plane (Figure 5a).

The inorganic $[Cu_8I_7]_n^{n+}$ motif contains eight independent Cu(I) atoms and seven I atoms. All Cu atoms adopt CuI_3N distorted tetrahedral geometries except for trigonal planar Cu(5) with a $Cu(5)I_2N$ configration. The Cu atoms are

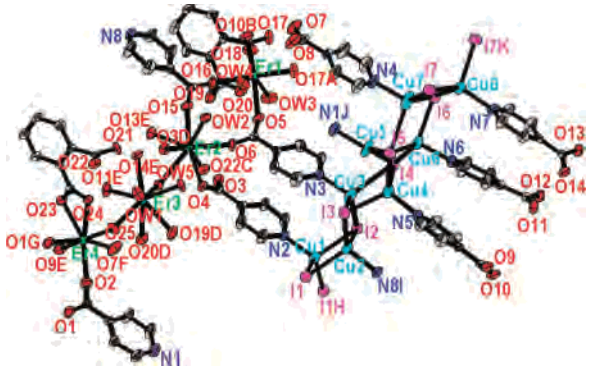

Figure 4. Coordination environments of Er and Cu atoms in **2**. Symmetry codes for the generated atoms are the same as in Table 3.

Table 3. Selected Bond Lengths (Å) for **2**[a]

Er(1)−O(16)	2.202(6)	Cu(2)−N(8I)	2.042(7)
Er(1)−O(5)	2.257(6)	Cu(2)−I(1)	2.6225(14)
Er(1)−O(18)	2.262(6)	Cu(2)−I(2)	2.6701(14)
Er(1)−O(17A)	2.279(6)	Cu(2)−I(3)	2.7246(15)
Er(1)−O(10B)	2.284(6)	Cu(2)−Cu(3)	2.8005(18)
Er(1)−OW3	2.317(7)	Cu(3)−N(3)	2.032(7)
Er(1)−OW4	2.394(6)	Cu(3)−I(3)	2.5970(14)
Er(2)−O(6)	2.273(5)	Cu(3)−I(2)	2.6309(15)
Er(2)−O(22C)	2.277(5)	Cu(3)−Cu(4)	2.7328(18)
Er(2)−O(3D)	2.278(5)	Cu(3)−I(4)	2.8087(15)
Er(2)−O(15)	2.315(6)	Cu(4)−N(5)	1.998(7)
Er(2)−O(13E)	2.336(6)	Cu(4)−Cu(5)	2.544(2)
Er(2)−O(4)	2.385(6)	Cu(4)−I(3)	2.5924(15)
Er(2)−OW2	2.405(6)	Cu(4)−I(4)	2.7129(15)
Er(2)−OW5	2.574(5)	Cu(4)−I(5)	2.8990(18)
Er(3)−O(25)	2.247(6)	Cu(4)−Cu(6)	3.004(2)
Er(3)−O(11E)	2.289(5)	Cu(5)−N(1J)	1.972(7)
Er(3)−O(21C)	2.321(5)	Cu(5)−I(4)	2.5763(16)
Er(3)−O(14E)	2.342(6)	Cu(5)−I(5)	2.6427(16)
Er(3)−O(19D)	2.344(7)	Cu(5)−Cu(6)	2.6772(18)
Er(3)−OW1	2.360(6)	Cu(6)−N(6)	2.019(7)
Er(3)−OW5	2.522(5)	Cu(6)−I(6)	2.6094(15)
Er(3)−O(20D)	2.612(6)	Cu(6)−I(5)	2.6376(14)
Er(4)−O(25)	2.202(6)	Cu(6)−Cu(7)	2.745(2)
Er(4)−O(7F)	2.237(6)	Cu(6)−I(4)	2.7903(15)
Er(4)−O(1G)	2.262(6)	Cu(7)−N(4)	2.042(7)
Er(4)−O(2)	2.262(6)	Cu(7)−I(6)	2.5503(17)
Er(4)−O(9E)	2.286(6)	Cu(7)−I(7)	2.6100(17)
Er(4)−O(23)	2.399(5)	Cu(7)−Cu(8)	2.839(2)
Er(4)−O(24)	2.430(6)	Cu(7)−I(5)	2.930(2)
Cu(1)−N(2)	2.048(6)	Cu(8)−N(7)	2.040(7)
Cu(1)−I(1)	2.6387(13)	Cu(8)−I(7)	2.6167(15)
Cu(1)−I(1H)	2.6735(14)	Cu(8)−I(7K)	2.6689(15)
Cu(1)−I(2)	2.7105(14)	Cu(8)−I(6)	2.7629(16)
Cu(1)−Cu(1H)	2.736(2)	Cu(8)−Cu(8K)	2.933(3)
Cu(1)−Cu(2)	2.8079(18)		

[a] Symmetry codes: (A) $-x+3, -y+2, -z+1$; (B) $x, y, z+1$; (C) $-x+2, -y+1, -z+1$; (D) $-x+2, -y+2, -z+1$; (E) $x-1, y, z+1$; (F) $x-1, y, z$; (G) $-x+1, -y+1, -z+1$; (H) $-x+2, -y+2, -z$; (I) $x, y, z-1$; (J) $x+1, y, z$; (K) $-x+4, -y+1, -z$; (L) $x+1, y, z-1$.

bridged by μ_3-I and μ_4-I to form a 1D $[Cu_8I_7]_n^{n+}$ motif with stairlike double chain (Figure 5b,c) that further links the adjacent Ln−organic layered motifs to produce the 3D framework (Figure 6).

Structure of 3. Compound **3** was made analogously to **1** by only replacing pdc with the bdc. In the structure of **3**, a 1D $[Cu_6Br_6]_n$ chainlike motif inserts into the channels of a 3D Ln−Cu−organic motif. The asymmetric unit of **3** contains three Ce^{3+}, seven Cu^+, and six Br^- ions, one bdc ligand, and eight ina ligands (Figure S3 and Scheme 1). The

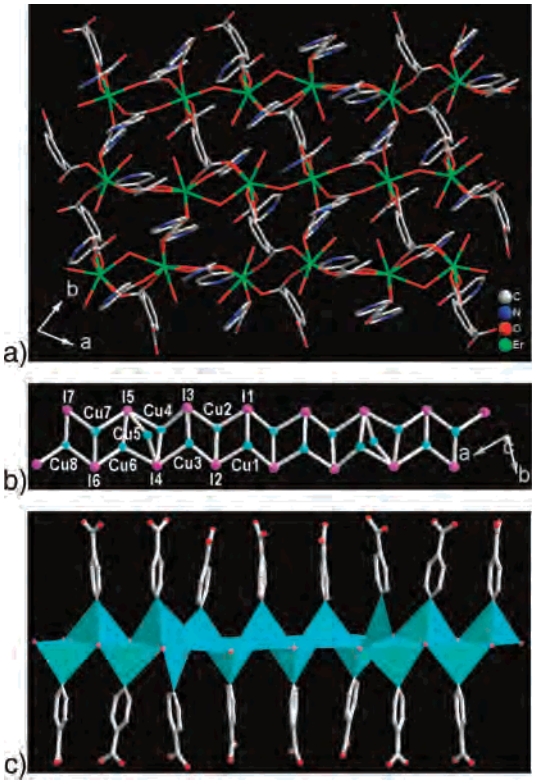

Figure 5. (a) Ln−organic layered motif in **2**. (b) Inorganic $[Cu_8I_7]_n^{n+}$ chains parallel to the *ab*-plane. (c) Polyhedral view of the 1D $[Cu_8I_7N_8]_n^{n+}$ chains.

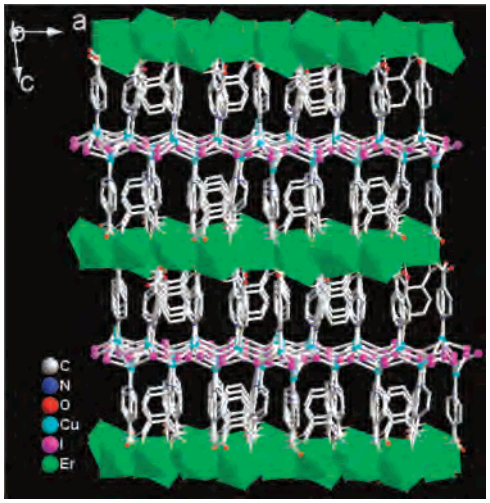

Figure 6. Framework of **2** viewed down the approximate [010] direction.

Ce(1) atom is nine-coordinate with tricapped trigonal prism geometry: two water molecules, five O_{COO}^- from five ina ligands, two O_{COO}^- from one bdc ligand for Ce(1). The Ce(2) and Ce(3) atoms are eight-coordinate with bicapped trigonal prism configurations: one water molecules, five O_{COO}^- from five ina ligands, two O_{COO}^- from one bdc ligand for Ce(2); one water molecules, six O_{COO}^- from six ina ligands, one $O_{COO\_}$ from one bdc ligand for Ce(3) (Figure 7, S3). The Ce−O bond lengths range from 2.389(6) to 2.798(6) Å (Table 4).

The inorganic $[Cu_6Br_6]_n$ motif contains six unique Cu(I) ions with three configrations and six Br^- ions; Cu7 is two-coordinated made up of Cu(7)BrN and the Cu(2,4,5) atoms

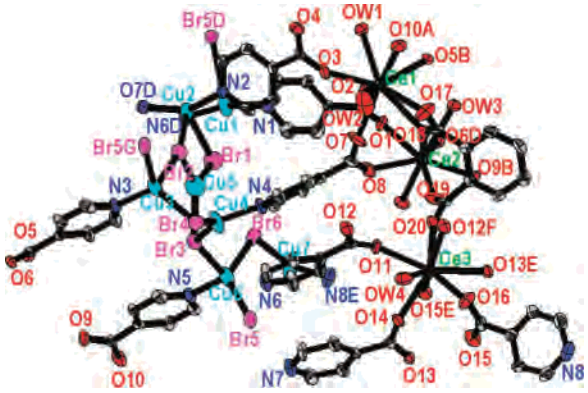

Figure 7. Coordination environments of Ce and Cu atoms in **3**. Symmetry codes for the generated atoms are the same as in Table 4.

Table 4. Selected Bond Lengths (Å) for **3**[a]

Ce(1)−O(10A)	2.393(6)	Cu(1)−N(1)	1.935(8)
Ce(1)−O(3)	2.426(7)	Cu(2)−Cu(2)	0.702(10)
Ce(1)−O(7)	2.427(7)	Cu(2)−N(7D)	1.958(8)
Ce(1)−O(2)	2.446(7)	Cu(2)−N(2)	1.976(8)
Ce(1)−O(17)	2.519(7)	Cu(2)−Br(1)	2.635(3)
Ce(1)−O(5B)	2.573(6)	Cu(2′)−N(2)	1.948(13)
Ce(1)−OW2	2.628(9)	Cu(2′)−N(7D)	1.980(13)
Ce(1)−OW1	2.663(7)	Cu(2′)−Br(2)	2.683(13)
Ce(1)−O(18)	2.798(6)	Cu(3)−N(3)	2.004(8)
Ce(2)−O(9B)	2.389(6)	Cu(3)−Br(4)	2.441(2)
Ce(2)−O(19)	2.396(7)	Cu(3)−Br(2)	2.496(2)
Ce(2)−O(4C)	2.435(6)	Cu(3)−Br(5G)	2.556(2)
Ce(2)−O(1)	2.452(6)	Cu(4)−N(4)	2.008(8)
Ce(2)−O(18)	2.473(6)	Cu(4)−Br(4)	2.3482(18)
Ce(2)−O(8)	2.514(7)	Cu(4)−Br(3)	2.3805(18)
Ce(2)−OW3	2.612(6)	Cu(4)−Cu(5)	2.750(3)
Ce(2)−O(6D)	2.618(6)	Cu(5)−Br(2)	2.290(3)
Ce(3)−O(15E)	2.418(7)	Cu(5)−Br(1)	2.331(2)
Ce(3)−O(12F)	2.433(6)	Cu(5)−Br(3)	2.350(2)
Ce(3)−O(11)	2.444(6)	Cu(6)−N(5)	2.035(8)
Ce(3)−O(20)	2.460(6)	Cu(6)−Br(5)	2.449(2)
Ce(3)−O(16)	2.488(7)	Cu(6)−Br(6)	2.452(2)
Ce(3)−O(14)	2.495(6)	Cu(6)−Br(3)	2.649(2)
Ce(3)−O(13E)	2.554(6)	Cu(6)−Cu(7)	2.723(2)
Ce(3)−OW4	2.705(7)	Cu(7)−N(8E)	1.930(9)
Cu(1)−N(6)D	1.931(8)	Cu(7)−Br(6)	2.228(2)

[a] Symmetry codes: (A) $x-1, -y+1/2, z-1/2$; (B) $x, -y+1/2, z-1/2$; (C) $x+1, y, z$; (D) $-x+1, y-1/2, -z+1/2$; (E) $-x+2, -y+1, -z$; (F) $-x+1, -y+1, -z$; (G) $x-1, y, z$; (H) $-x+1, y+1/2, -z+1/2$; (I) $x, -y+1/2, z+1/2$; (J) $x+1, -y+1/2, z+1/2$.

have trigonal configrations of $Cu(2)BrN_2$, $Cu(4)Br_2N$, and $Cu(5)Br_3$, while the Cu(3,6) atoms show distorted tetrahedral geometries made of $CuBr_3N$. The Cu^+ ions extends along the *a*-axis by μ_2-Br and μ_3-Br to form a unique $[Cu_6Br_6]_n$ chainlike motif (Figure 8c,d). Three identical Ce ions are linked by ina and bdc ligands to give a 2D Ln−organic layer in the *ab* plane which differs from that in **2** and is further extended by the bridging $[Cu(1)(ina)_2]^-$ (Figures 8a and S3), forming a 3D 3d−4f pillared-layer metal−organic motif with 1D channels (Figure 8b) where the inorganic $[Cu_6Br_6]_n$ motifs are located (Figure 9). It is interesting to note that Cu^+ is two-coordinated with nonlinear $Cu(ina)_2^-$ in a geometry that is rare. Although Cu^{2+} ions were used as starting materials in **1** and **3**, the Cu centers have an oxidation state of +1, attributed to a reduction reaction involving the ina ligands, and is consistent with the geometry of the Cu^+ ions.

Compounds **1**−**3** exhibit different metal−organic motifs by introducing mixed ligands. The structural variability of

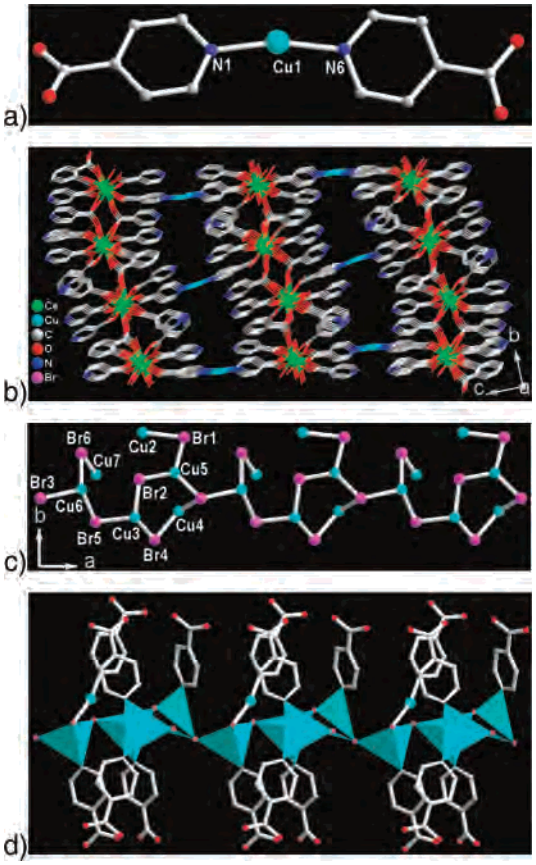

Figure 8. (a) Near linear coordination environments of the Cu1 atom. (b) 3D Ln−Cu−organic framework in 3. (c) Inorganic $[Cu_6Br_6]n$ chains along the a-axis. (d) Polyhedral view of the 1D $[Cu_6Br_6N_6]_n$ chains.

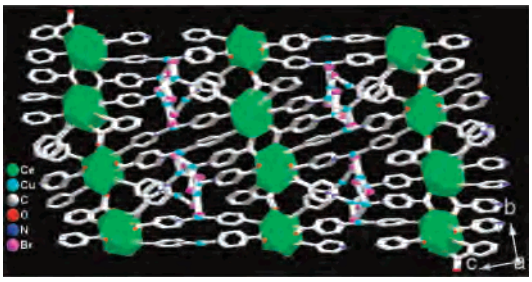

Figure 9. Framework of **3** viewed down the approximate [100] direction.

the frameworks, three different unreported 1D inorganic copper halide chainlike motifs interconnected with the 1-, 2-, and 3D metal−organic motifs, indicates a synergism between the metal−organic motif and inorganic copper halide motif at the organic−inorganic interface. The different ionic radius of halogen atoms may influence the shape of metal halide chains. It is interesting to note that copper halide chains exhibits short Cu···Cu distances shorter than the double van der Waals radius of the Cu(I) ion (1.4 Å) in the cluster subunits (Tables 2−4), indicating a strong Cu−Cu interaction. In addition, the architectures of **1**−**3** are not maintained across the whole lanthanide series as the ionic radii of rare earth cations decrease with increasing atomic number (lanthanide contraction), which imposes evident influence on the coordination geometry and might lead to other types of structure with different lanthanide ions.

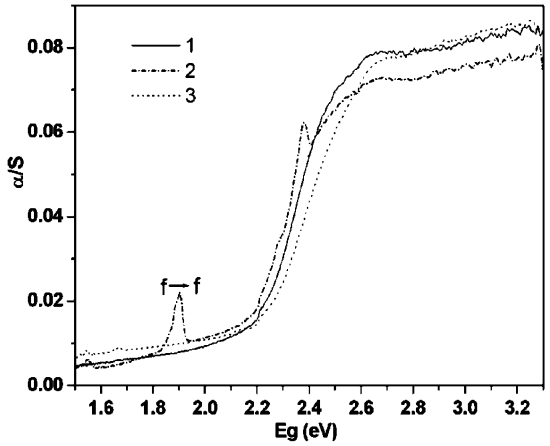

Figure 10. Optical absorption spectra for solid samples of **1**−**3**.

The thermal stabilities of **1**−**3** were examined by TG analysis in dry air atmosphere from 30 to 1000 °C. These compounds show similar thermal behavior and undergo two steps of weight loss. The coordinated water molecules were gradually lost in the temperature range 140−240 °C for **1** (calcd/found: 2.0/2.3%), 160−250 °C for **2** (calcd/found: 2.6/3.2%), and 170−260 °C for **3** (calcd/found: 2.8/2.9%), respectively. Above that temperature range, the weight loss is due to the decomposition of the organic ligandss and the collapse of the whole framework (Figure S4).

The IR spectra of **1**−**3** are similar. The strong and broad absorption bands in the range 3000−3700 cm^{-1} in **1**−**3** are assigned as characteristic peaks of OH vibration. The strong vibrations appearing around 1598 and 1410 cm^{-1} correspond to the asymmetric and symmetric stretching vibrations of the carboxylate group, respectively. The absence of strong bands ranging from 1690 to 1730 cm^{-1} indicates the ligands are deprotonated (Figure S5).

Encouraged by the single-crystal diffraction result, which reveals the presence of 1D copper halide chains being further linked by Ln−organic motifs in the framework, we measured the optical diffuse reflectance spectra of **1**−**3** in the solid state. Optical absorption spectra revealed that **1**−**3** exhibit strong and similar optical absorption in the visible region, with optical band gaps of 2.23, 2.21, and 2.25 eV, respectively. These band gap sizes are significantly smaller than that of CuBr and CuI (Figures 10 and S6). Thus, a much larger fraction of visible light is absorbed by these Ln-containing heterometallic compounds. The narrow spectral lines in **2** are attributed to the f−f transitions of Er^{3+}.[14]

Conclusion

In summary, we have made three novel 3D heterometallic coordination polymers under hydrothermal conditions, each with two distinct non-interpenetrating motifs, inorganic CuX chains, and 1D/2D/3D metal−organic frameworks. The key points of the synthetic procedures have been well established, which represent good examples and a facile method to construct such mixed-motif heterometallic compounds. By

(14) Zeng, H.; Mattausch, H.; Simon, A.; Zheng, F.; Dong, Z.; Guo, G.; Huang, J. *Inorg. Chem.* **2006**, *45*, 7943.

further changing the metal−organic parts with different ligands, different sizes and shapes of the inorganic copper halide subunits with various dimensions could be expected. This work opens new perspectives for the construction of fascinating mixed-motif Ln−TM networks, and work is continuing in this area.

Acknowledgment. This work was supported by the National Natural Science Fund for Distinguished Young Scholars of China (Grant No. 20725101), the NNSF of China (Grant No. 20473093), the 973 Program (Grant No. 2006CB932904), and the NSF of Fujian Province (Grant No. E0510030).

Supporting Information Available: X-ray crystallographic files in CIF format for structures **1**−**3**, IR spectra, UV−visible spectra, and TG curves. This material is available free of charge via the Internet at http://pubs.acs.org.

IC701468Q